The Effect of Polarity and Current Strength on Multilayer Wire Arc Additive Manufacturing (WAAM) Based Tungsten Inert Gas (TIG) Welding using ER5356 and ER1100 Welding Wire on SS316 Plates

Agus Sentana
Mechanical Engineering Department, Faculty of Engineering, Universitas Indonesia

Morryana Firman Firdaus Subki
Mechanical Engineering Department, Faculty of Engineering, Universitas Indonesia

Mohammad Azwar Amat
Mechanical Engineering Department, Faculty of Engineering, Universitas Indonesia

Ario Sunar Baskoro
Mechanical Engineering Department, Faculty of Engineering, Universitas Indonesia

他

https://doi.org/10.5109/7326969

出版情報：Evergreen. 11 (4), pp.3341-3347, 2024-12. 九州大学グリーンテクノロジー研究教育センター
バージョン：

The Effect of Polarity and Current Strength on Multilayer Wire Arc Additive Manufacturing (WAAM) Based Tungsten Inert Gas (TIG) Welding using ER5356 and ER1100 Welding Wire on SS316 Plates

Agus Sentana, Morryana Firman Firdaus Subki, Mohammad Azwar Amat, Ario Sunar Baskoro*, Gandjar Kiswanto
Mechanical Engineering Department, Faculty of Engineering, Universitas Indonesia, Depok, Indonesia

*Author to whom correspondence should be addressed:
E-mail: ario@eng.ui.ac.id

(Received October 22, 2023; Revised July 31, 2024; Accepted November 25, 2024).

Abstract: The additive manufacturing process can be carried out with a welding-based process. The welding process that can be used to manufacture metal products or components with arc welding technology is Tungsten Inert Gas (TIG) welding. This study presents the effect of current and polarity on multilayer WAAM-based TIG welding with ER 5356 and ER 1100 filler materials on SS316 base plates. The influence of current and polarity in TIG welding is evident from the weld bead's geometry, appearance, and quality. The experimental results of the welding bead on DC polarity are more consistent than those on AC polarity.

Keywords: Polarity; Current; Welding wire; Wire Arc Additive Manufacturing; TIG Welding

1. Introduction

Advances in science and technology have increased the demand for welding technology to meet current industrial needs. Metal welding is an essential manufacturing process in the development of the industrial world. Some examples of industries are airplanes, shipping, automotive applications, Etc[1,2]. The sector requires metal joints with excellent quality so that the products produced are safe and meet standards. The study of metal welding is often carried out mainly focusing on the materials used, composition, and mechanical properties of the workpiece, as well as all process parameters that affect efficiency and product quality. The development of welding technology, in addition to meeting the needs of joints, can also be used to manufacture products. Making products with metal materials still uses a casting process where the final product still requires much machining. This, of course, requires more power, expensive production costs, and a long production time. Many studies have optimized metal production processes, one of which is additive manufacturing technology. Additive manufacturing (AM) is known as 3D printing and is considered a significant innovation in manufacturing technology in the 20th century, which is highly valued by many countries. M. Nazmi et al. researched the performance results of stacks made using 3D printing technology that minimizes errors, eliminates deviations and can reduce production time[3]. The main factors influencing the choice of welding process in the manufacture of additives are the complexity and resolution that can be achieved, as well as the degree of deposition and the size of the components[4]. Additionally, additive manufacturing provides more freedom for product design than conventional manufacturing processes and opens design opportunities with load optimization. One promising area of additive manufacturing processes is wire arc additive manufacturing (WAAM), where an electric arc combined with wire as a precipitating agent is used to manufacture a product. The process of DED includes a nozzle head capable of focusing the thermal source and feeding material into a single unit, providing a more economical additive manufacturing method[5]. This additive manufacturing process is part of Direct Energy Deposition (DED) manufacturing. As of 2020, Direct Energy Deposition (DED) technologies represent 16% of additive manufacturing used in the market. Material cost is reduced to 7–69% with the WAAM technique. Reduction in fabrication time is around 40–60% and reduction in post-machining time is around 15–20%[6,7]. The MIG-based additive manufacturing process is used by most researchers over the GTAW welding-based additive manufacturing process because it has the highest deposition rate and makes it easier to synchronize the wire feed with the heat source. Whereas the GTAW weld-based additive manufacturing process has a high deposition rate

(although less than MIG), is spatter-free, and has high thermal efficiency 68%[8]. Benakis et al. demonstrated that the slow, inter-pulsed TIG welding process has a good melt pool shape for additive manufacturing[9]. The WAAM process has challenges that must be mastered for defect-free and geometrically correct parts manufacturing. The uneven solidification of the molten metal results in residual stress which is a kind of defect and is shown in the form of crack. Additionally, porosity is a common problem during most processing aluminum alloys and should be avoided or kept as low as possible. Porosity, mainly due to gas entrapment, is the most common defect in WAAM[10,11]. Heziqi Liu et al., investigated the effects of different arc modes on pore formation, microstructural characteristics, and tensile properties. High-frequency pulse current and cyclic polarity reversal in CMT-PADV mode proved beneficial for reducing pores[12]. There is wall height prediction in path planning, design distance between weld bead and directional weld point, and single bead sequence. Besides that, the development of AM for the fabrication of multi-material has improved the mechanical properties, specific functional requirements and design features of the new product[13].

Fabrication time is one of the important factors for considering the WAAM method. Fabrication time mainly depends on the speed of welding in the WAAM process[14]. Generally, the selection of welding parameters is carried out by trial and error, but as technology advances, the prediction of welding parameters is becoming increasingly model-based[4]. The current and polarity are parameters that influence the formation of weld beads. Chen Shen et al. indicated that welding wire deposition is influenced by current and is the dominant factor in the grain size of the weld bead wall buildup[15]. The grain size increases as the wire feed speed increases, heat input increases, and travel speed constantly due to solidification rate decrease. In contrast, travel speed increase and others remain constant, resulting in faster solidification and slow down the grain growth rate[16].

This research will discuss the influence of polarity and current on Tungsten Inert Gas (TIG) welding based on wire arc additive manufacturing (WAAM) using welding wire (filler) ER5356 and ER 1100 in a multilayer or layer-by-layer deposition process. The results of this research study analyze the success rate of the weld metal deposition process layer by layer using visual and testing methods such as weld bead appearance, weld bead geometry and dimensions.

2. Material and Method

The base metal or substrate used in this study is a Stainless Steel 316 plate which has a thickness of 5 mm a length of 150 mm and a width of 50 mm using welding wire ER-5356 and ER 1100 diameter 1.2 mm. In this study, a TIG welding experiment was carried out using an automatic or intermittent wire feeder welding method with filler metal ER5356 and ER 1100 on a 316 stainless steel plate by varying the current and polarity[17,18]. Gokhale et al. discuss the effect of wire feeders or wire feeders on welding metal deposition. The scheme of the wire feeding method used in their study found that a smoother surface appearance was observed when the wire feeding nozzle made a smaller angle of about 13°–15° with the substrate plate[8]. The welding torch and filler metal are generally kept inclined at angles of 700– 800 and 10-20 degrees respectively with the flat workpiece. The research results of Elif Karayel et al., show that the influence of the torch angle to the workpiece, an angle of 80◦ is a better choice and as the inclination angle increases, the deposition will increase, the width will increase, and the deposition height will decrease[19]. Haochen Mu et al., in their research regarding the design chosen for controlling weld bead geometry, namely wire feeding speed (WFS) and travel speed (TS)[20]. Lower TS entails larger molten pool volumes for the same arc pressure (same current and arc length), making the weld pool more prone to lateral sagging and resulting in irregularities[21].

The Experiments were carried out by observing the results of the weld bead in first layer and second layers. Retrieval of this data is to see and get TIG welding results with neat and unblemished shapes and geometries. Bead width, bead height, molten metal depth, and wetting angle were measured to observe the effect of process parameters on the resulting geometry. Measurements were performed using ImageJ or Dino-Lite[22]. Determination of parameters is carried out in addition to experimental design and through several trials. From the geometry, dimensions and appearance data of the weld bead, current and polarity parameters can be obtained which influence the quality of the weld bead. Within welding parameters, welding polarity has a significant effect on temperature distribution in weldments which affects the microstructure, mechanical properties and residual stresses distribution of components considerably[23]. Increasing the heat input is affected by the arc current, and for a higher current, the wire feed volume increases. Unlike the voltage, the WFS increases, thus, the material deposition volume per layer also increases[24].

The equipment used in this research included a Miller Dynasty 210 DX Tungsten Inert Gas (TIG) welding machine, power source, wire feeder, tungsten electrode, torch and controller shown in Fig. 1. The polarities used in the WAAM process with TIG welding are DC and AC polarities. The initial holding or heating time is 15 seconds so the temperature or heat is even. The current used varies, namely 120A, 130A, 140A, 150A, 160A, and 170A, with a constant argon gas flow rate of 11 L/minute and a continuous welding speed of 3.125 mm/s with a welding time of 30 seconds. Problems that may arise with multilayer weld beads are cracking and delamination. This cannot be corrected by post-processing treatment, so pre-processing treatments, such as pre-heating the substrate[25]. The configuration parameter was influenced by welding speed, wire feeding speed, feeding time, and delaying

time[26]. The high-angle wire feeding has been demonstrated as an effective way to get uniform deposition in any wire feeding direction[27]. The angle between each nozzle and the substrate surface is 30° to ensure the stability of molten pool[15]. For multi-layer weld beads, as the number of layers increases, the weld bead offset will gradually decrease[28].

The following is a test setup for the TIG welding process based on wire arc and additive manufacturing (WAAM) which can be seen in Fig. 2.

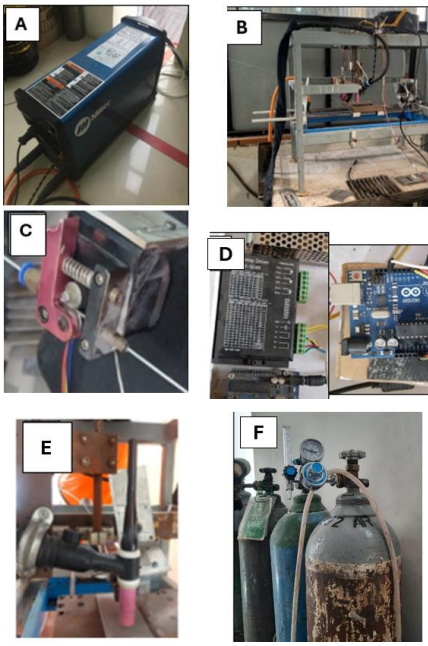

Fig. 1: Equipment used in WAAM-based TIG welding (A) Miller Dynasty 210 DX welding machine, (B) Machine construction, (C) Wire feeder, (D) Motor driver and Arduino, (E) Torch welding, (F) Argon gas cylinder.

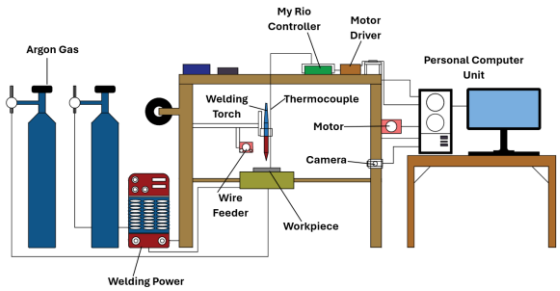

Fig. 2: The setup of testing the WAAM-based TIG welding.

The welding process parameters used in the WAAM-based TIG welding experiment can be seen in Table 1 below. Use the following table format in the manuscript. Note that all the tables and figures should be cited in the paragraph as Table 1 and Fig. 1 where appropriate.

Table 1. WAAM based TIG welding process parameters.

Process parameter	
Welding current, A	50 - 170
Welding speed, mm/min	187.5
Pre-heating time, s	15
Constant parameter	
Arc voltage	13
Frequency, Hz	250
Electrode diameter, mm	2.4
Shielding gas type	Pure Argon
Flow rate, L/mm	11
Filler wire type	ER 5356
Filler diameter, mm	1.2
Wire feeder speed, mm/s	3.125
Wire feeder angle, Θ	15^0
Wire feeder method	intermittent

3. Result and Discussion

TIG welding results with the application of specific current and polarity parameters can be seen visually and by measuring the geometry and dimensions of the weld bead. The weld bead geometry measures the top bead width and the weld bead[29]. Measurement data were obtained from 6 specimens on the first layers and second layers. Good quality TIG welding beads in layers one will be used as the foundation for layers two and subsequent layers. Defect in WAAM product is typically severe oxidation in titanium alloys, porosity in aluminum alloys, poor surface roughness in steel, and severe deformation and cracks in nickel alloys[30]. The main reasons for obtaining defects in WAAM of aluminum alloys are an inappropriate selection of parameters, the bad strategy of programming, and unsteady weld pools[31].

3.1 First Layer using Filler ER 5356 AC Polarity

The experimental results with DC polarity ER5356 filler produced a dirty surface, but the resulting weld bead was entirely consistent because the current increased from 120A to 160A. From the measurement and observation results, the 160A current produces the neatest bead with a flat and uniform weld bead surface, compared to using other currents, as shown in Fig. 3. Thus, the weld bead that can be used as a foundation for the next layer is the weld bead of TIG welding results at a current of 160A with a break for 15 seconds.

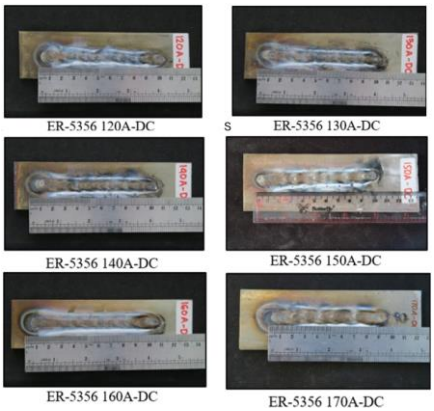

Fig. 3: TIG welding results using filler ER5356 DC polarity.

The following data results from measuring the width of the weld bead for filler ER 5356 with DC polarity using the Dino-Lite digital microscope shown in Fig. 4.

During the initial layer deposition, heat input was controlled with high amperage (110–140 A). For higher layer depositions, weld velocity was varied to control the heat input[32].

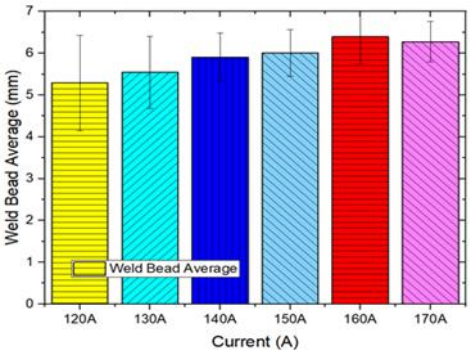

Fig. 4: Correlation of average weld bead width with current for DC polarity.

In the layer 2 experiment, AC polarity was used and tested for currents starting from 100A, 110A, 120A, 140A, 150A, and 160A, as shown in Fig. 5.

Fig. 5: TIG welding results using filler ER5356 AC polarity.

The results of first layer and second layer with different polarities show that the geometry of the weld bead is not neat, there are lumps of weld metal, the weld bead is broken, and there are also crack defects that can occur due to solidification cracking process and residual stresses. That temperature is a function of the deposition of electrical current[33]. Non-uniform expansion and shrinkage in the fusion zone of weld is not only the reason for distortion in assembly of components but other controllable parameters are also very significant and should be considered in weld planning[34].

3.2 First Layer using Filler ER 1100 DC polarity

The experimental results using ER 1100 filler showed that the weld bead had a constant geometry and relatively no defects at a current of 135 A, a welding speed of 3.125 cm/s, and an argon flow rate of 11 lt/min. The following are the experimental results shown in Fig. 6.

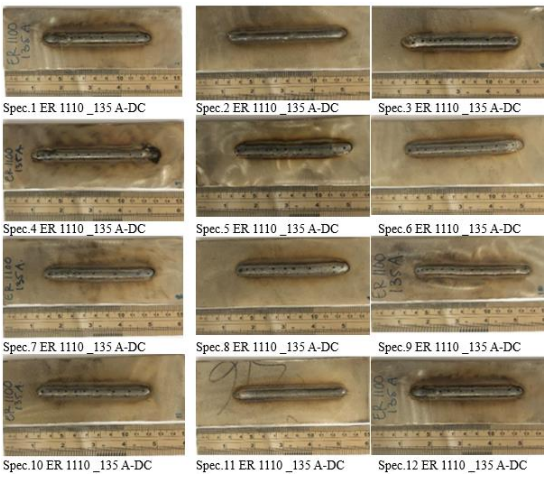

Fig. 6: First layer welding bead at 135 A current filler ER1100 with DC polarity.

3.3 First Layer using Filler ER 1100 DC polarity

Welding using AC polarity on ER1100 filler shows cleaner results than DC polarity, but the resulting weld beads are inconsistent, as shown in Fig. 7.

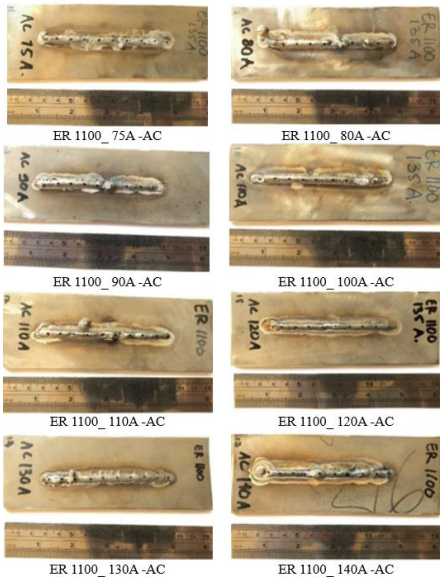

Fig. 7: Second layer welding bead (75A to 140A) filler ER1100 with AC polarity.

The bead height behavior tends to increase as the welding wire feeding speed increases, which also increases vice versa; if the current parameter increases or increases, the weld bead height will decrease. Figure 8 shows that something unusual when the current increases in some tests; bead height also increases. This is presumably due to varying electric current intensities and disturbances or noise during the welding process[35].

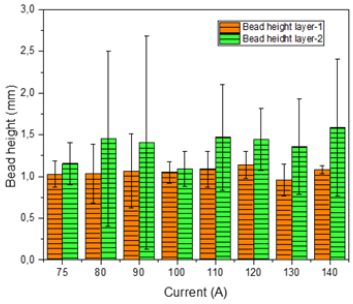

Fig. 8: Comparison of the height of the first weld bead layer with the second layer of ER 1100 filler-AC Polarity.

The heat input and energy density increase with current, consequently increasing the amount and temperature of the molten metal, and the resulting bead will have an increased width.

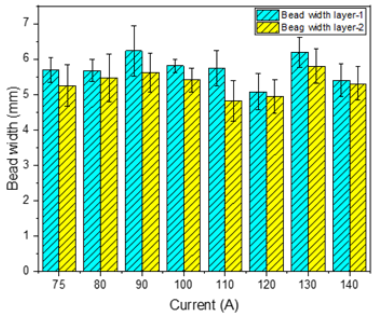

Fig. 9: Comparison of the width of the first weld bead layer with the second layer of ER 1100 filler-AC polarity.

The width of the bead tends to increase in direct proportion to the increase in current, as shown in Fig. 9. The influence of heat input on the surface quality of additive manufacturing arc sections is analyzed by changing the welding current and speed or travel speed. Higher heat input represents sufficient heat, which can not only make the weld pool take a better shape on the surface of the substrate during WAAM but also has a better stabilizing effect on the weld pool[36].

3.4 Second layer using Filler ER 1100 DC polarity

Below in Fig. 10 are weld beads from experiments on the second layer of DC polarity with a current range from 120A to 160A using ER 1100 welding wire.

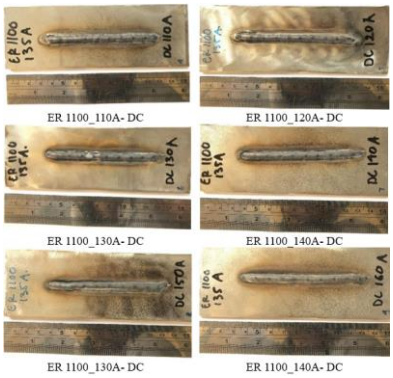

Fig. 10: Second layer welding bead (110A to 160A) filler ER1100 with DC polarity.

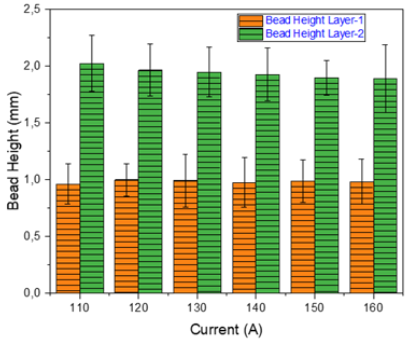

Fig. 11: Comparison of the height of the first weld bead layer with the second layer of ER 1100 filler DC polarity.

Research by Xiaoxuan C. et al. shows that the heat input gradually increases, the thickness of the printed layer increases, and the number and size of pores in the deposit also improve, which is by Fig. 11[37].

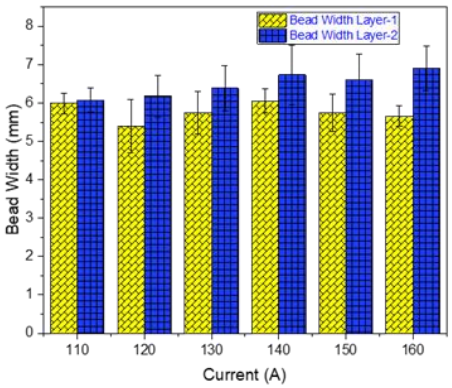

Fig. 12: Comparison of the width of the first weld bead layer with the second layer of ER 1100 filler DC polarity.

Figure 12 shows that the comparison of the second layer weld bead width is greater than the first layer and is relatively comparable for several welding current prices. At a welding current of 110A DC polarity, the width of the weld bead is relatively the same as that of the first and second layers. In the specimens of multiple layers, no observable interface between the layers was present, suggesting a complete fusion between layers with no oxidation[38].

4. Conclusion

According to the results shown above, the conclusions are as follows:

1. The effect of current and polarity that occurs in TIG welding with the ER 5356 filler can be seen in the geometry and appearance of the weld bead, and the greater the current, the wider the geometry of the weld bead.
2. The heat input and energy density increase with current, consequently increasing the amount and temperature of the molten metal and the resulting bead will have an increased width.
3. Increasing the current causes an increase in the weld bead width even though the rate of decrease is

relatively small. Meanwhile, in the first layer, the weld bead width tends to be inconsistent.

4. Welding using AC polarity on the ER1100 filler, the macrostructure and weld bead geometry appear more continuous and cleaner the DC polarity.
5. The test results show that the weld bead second layer that is suitable and has consistent geometry and a pleasing appearance is a TIG welding process with DC polarity.

Acknowledgements

This research is supported by the Hibah Penelitian Fundamental Reguler Year 2023 Program from the Ministry of Education, Culture, Research and Technology. Republic of Indonesia, with contract number: No. NKB-1141/UN2.RST/HKP.05.00/2023.

References

1) Y. Li, C. Su, and J. Zhu, "Comprehensive review of wire arc additive manufacturing: hardware system, physical process, monitoring, property characterization, application and future prospects," *Results Eng.*, **13** (*December 2021*) 100330 (2022). doi:10.1016/j.rineng.2021.100330.
2) J. Kumaraswamy, K.C. Anil, T.R. Veena, G. Purushotham, and S.K. K, "Investigating the mechanical properties of al 7075 alloy for automotive applications : synthesis and analysis," *Evergreen*, **10** (*03*) 1286–1295 (2023).
3) M.N.H. Roslan, N.A. Zolpakar, N. Mohd-Ghazali, and F.A.Z.M. Saat, "Analysis of 3d printed stack in thermoacoustic cooling," *Evergreen*, **8** (*1*) 131–137 (2021). doi:10.5109/4372269.
4) K. Treutler, and V. Wesling, "The current state of research of wire arc additive manufacturing (waam): a review," *Appl. Sci.*, **11** (*18*) (2021). doi:10.3390/app11188619.
5) M.R. Zahidin, F. Yusof, S.H. Abdul Rashid, S. Mansor, S. Raja, M.F. Jamaludin, Y.H. Manurung, M.S. Adenan, and N.I. Syahriah Hussein, "Research challenges, quality control and monitoring strategy for wire arc additive manufacturing," *J. Mater. Res. Technol.*, **24** 2769–2794 (2023). doi:10.1016/j.jmrt.2023.03.200.
6) K.E.K. Vimal, M. Naveen Srinivas, and S. Rajak, "Wire arc additive manufacturing of aluminium alloys: a review," *Mater. Today Proc.*, **41** (*xxxx*) 1139–1145 (2019). doi:10.1016/j.matpr.2020.09.153.
7) B. Tomar, S. Shiva, and T. Nath, "A review on wire arc additive manufacturing: processing parameters, defects, quality improvement and recent advances," *Mater. Today Commun.*, **31** (*January*) 103739 (2022). doi:10.1016/j.mtcomm.2022.103739.
8) N.P. Gokhale, P. Kala, and V. Sharma, "Thin-walled metal deposition with gtaw welding-based additive manufacturing process," *J. Brazilian Soc. Mech. Sci. Eng.*, **41** (*12*) 1–12 (2019). doi:10.1007/s40430-019-2078-z.
9) M.J. Bermingham, J. Thomson-Larkins, D.H. St John, and M.S. Dargusch, "Sensitivity of ti-6al-4v components to oxidation during out of chamber wire + arc additive manufacturing," *J. Mater. Process. Technol.*, **258** 29–37 (2018). doi:10.1016/j.jmatprotec.2018.03.014.
10) T. Hauser, R.T. Reisch, P.P. Breese, B.S. Lutz, M. Pantano, Y. Nalam, K. Bela, T. Kamps, J. Volpp, and A.F.H. Kaplan, "Porosity in wire arc additive manufacturing of aluminium alloys," *Addit. Manuf.*, **41** (*February*) 101993 (2021). doi:10.1016/j.addma.2021.101993.
11) D. Svetlizky, M. Das, B. Zheng, A.L. Vyatskikh, S. Bose, A. Bandyopadhyay, J.M. Schoenung, E.J. Lavernia, and N. Eliaz, "Directed energy deposition (ded) additive manufacturing: physical characteristics, defects, challenges and applications," *Mater. Today*, **49** (*October*) 271–295 (2021). doi:10.1016/j.mattod.2021.03.020.
12) H. Liu, K. Hao, L. Xu, Y. Han, L. Zhao, and W. Ren, "Effect of arc mode on laser-arc hybrid additive manufacturing of al–cu alloy: pore defects, microstructure and mechanical properties," *Mater. Sci. Eng. A*, **891** (*September 2023*) 146022 (2024). doi:10.1016/j.msea.2023.146022.
13) N.K. Maurya, V. Rastogi, and P. Singh, "Experimental and computational investigation on mechanical properties of reinforced additive manufactured component," *Evergreen*, **6** (*3*) 207–214 (2019). doi:10.5109/2349296.
14) M.N. Srinivas, and K.E.K.V.N. Manikandan, "Parametric optimization and multiple regression modelling for fabrication of aluminium alloy thin plate using wire arc additive manufacturing," *Int. J. Interact. Des. Manuf.*,(2022). doi:10.1007/s12008-022-00921-1.
15) C. Shen, Z. Pan, D. Cuiuri, D. Ding, and H. Li, "Influences of deposition current and interpass temperature to the fe3al-based iron aluminide fabricated using wire-arc additive manufacturing process," *Int. J. Adv. Manuf. Technol.*, **88** (*5–8*) 2009–2018 (2017). doi:10.1007/s00170-016-8935-3.
16) N. Ana, M. Rizal, M. Fadzli, S. Maidin, F. Redza, and S. Gazali, "Review on effect of heat input for wire arc additive manufacturing process," *J. Mater. Res. Technol.*, **11** 2127–2145 (2021). doi:10.1016/j.jmrt.2021.02.002.
17) A.S. Baskoro, M.A. Amat, S.P.D. Simatupang, Y. Abrara, and A. Widyianto, "Weld geometry, mechanical properties, microstructure and chemical composition of aa6063 in tungsten inert gas welding with intermittent controlled wire feeding method," *Metals (Basel).*, **11** (*2*) 1–14 (2021). doi:10.3390/met11020316.

18) A.S. Baskoro, M.A. Amat, A.I. Pratama, G. Kiswanto, and W. Winarto, "Effects of tungsten inert gas (tig) welding parameters on macrostructure, microstructure, and mechanical properties of aa6063-t5 using the controlled intermittent wire feeding method," *Int. J. Adv. Manuf. Technol.*, **105** (*5–6*) 2237–2251 (2019). doi:10.1007/s00170-019-04400-y.
19) E. Karayel, and Y. Bozkurt, "Additive manufacturing method and different welding applications," *J. Mater. Res. Technol.*, **9** (*5*) 11424–11438 (2020). doi:10.1016/j.jmrt.2020.08.039.
20) H. Mu, J. Polden, Y. Li, F. He, C. Xia, and Z. Pan, "Layer-by-layer model-based adaptive control for wire arc additive manufacturing of thin-wall structures," *J. Intell. Manuf.*, **33** (*4*) 1165–1180 (2022). doi:10.1007/s10845-022-01920-5.
21) F.R. Teixeira, F.M. Scotti, L.O. Vilarinho, C.A.M. da Mota, and A. Scotti, "Transferability of the working envelope approach for parameter selection and optimization in thin wall waam," *Int. J. Adv. Manuf. Technol.*, **119** (*1–2*) 969–989 (2022). doi:10.1007/s00170-021-08326-2.
22) A.S. Baskoro, M.A. Amat, R.D. Putra, A. Widyianto, and Y. Abrara, "Investigation of temperature history, porosity and fracture mode on aa1100 using the controlled intermittent wire feeder method," *Evergreen*, **7** (*1*) 86–91 (2020). doi:10.5109/2740953.
23) A. Sarmast, and S. Serajzadeh, "The influence of welding polarity on mechanical properties, microstructure and residual stresses of gas tungsten arc welded aa5052," *Int. J. Adv. Manuf. Technol.*, **105** (*7–8*) 3397–3409 (2019). doi:10.1007/s00170-019-04580-7.
24) D. Jafari, T.H.J. Vaneker, and I. Gibson, "Wire and arc additive manufacturing: opportunities and challenges to control the quality and accuracy of manufactured parts," *Mater. Des.*, **202** 109471 (2021). doi:10.1016/j.matdes.2021.109471.
25) B. Wu, Z. Pan, D. Ding, D. Cuiuri, H. Li, J. Xu, and J. Norrish, "A review of the wire arc additive manufacturing of metals: properties, defects and quality improvement," *J. Manuf. Process.*, **35** (*February*) 127–139 (2018). doi:10.1016/j.jmapro.2018.08.001.
26) M.R.U. Ahsan, G.-J. Seo, X. Fan, P.K. Liaw, S. Motaman, C. Haase, and D.B. Kim, "Effects of process parameters on bead shape, microstructure, and mechanical properties in wire + arc additive manufacturing of al0.1cocrfeni high-entropy alloy," *J. Manuf. Process.*, **68** (*PA*) 1314–1327 (2021). doi:10.1016/j.jmapro.2021.06.047.
27) Q. Wu, J. Lu, C. Liu, X. Shi, Q. Ma, S. Tang, H. Fan, and S. Ma, "Obtaining uniform deposition with variable wire feeding direction during wire-feed additive manufacturing," *Mater. Manuf. Process.*, **32** (*16*) 1881–1886 (2017). doi:10.1080/10426914.2017.1364860.
28) X. Wang, A. Wang, and Y. Li, "Study on the deposition accuracy of omni-directional gtaw-based additive manufacturing," *J. Mater. Process. Technol.*, **282** (*January*) 116649 (2020). doi:10.1016/j.jmatprotec.2020.116649.
29) P. Gokhale Nitish, P. Kala, and V. Sharma, "Experimental investigations of tig welding based additive manufacturing process for improved geometrical and mechanical properties," *J. Phys. Conf. Ser.*, **1240** (*1*) (2019). doi:10.1088/1742-6596/1240/1/012045.
30) M. Navarro, A. Matar, S.F. Diltemiz, and M. Eshraghi, "Development of a low-cost wire arc additive manufacturing system," *J. Manuf. Mater. Process.*, **6** (*1*) 3 (2022). doi:10.3390/jmmp6010003.
31) M.M. Tawfik, M.M. Nemat-Alla, and M.M. Dewidar, "Enhancing the properties of aluminum alloys fabricated using wire + arc additive manufacturing technique - a review," *J. Mater. Res. Technol.*, **13** 754–768 (2021). doi:10.1016/j.jmrt.2021.04.076.
32) I. Ünsal, M. Hirtler, A. Sviridov, and M. Bambach, "Material properties of features produced from en aw 6016 by wire-arc additive manufacturing," *Procedia Manuf.*, **47** (*2019*) 1129–1133 (2020). doi:10.1016/j.promfg.2020.04.131.
33) A.F. Moreira, K.S.B. Ribeiro, F.E. Mariani, and R.T. Coelho, "An initial investigation of tungsten inert gas (tig) torch as heat source for additive manufacturing (am) process," *Procedia Manuf.*, **48** (*2019*) 671–677 (2020). doi:10.1016/j.promfg.2020.05.159.
34) P. Kumar, "Distortion analysis of mag welded is2062 steel structure," *Evergreen*, **10** (*2*) 1017–1026 (2023). doi:10.5109/6793657.
35) C.F. Schneider, C.P. Lisboa, R. de Almeida Silva, and R.T. Lermen, "Optimizing the parameters of tig-mig/mag hybrid welding on the geometry of bead welding using the taguchi method," *J. Manuf. Mater. Process.*, **1** (*2*) 1–17 (2017). doi:10.3390/jmmp1020014.
36) H. Bikas, P. Stavropoulos, and G. Chryssolouris, "Additive manufacturing methods and modeling approaches: a critical review," *Int. J. Adv. Manuf. Technol.*, **83** (*1–4*) 389–405 (2016). doi:10.1007/s00170-015-7576-2.
37) X. Chen, X. Shang, Z. Zhou, and S. Chen, "A review of the development status of wire arc additive manufacturing technology," *Adv. Mater. Sci. Eng.*, **Jan 2022** (*1*) 28 (2022). doi:10.1155/2022/5757484.
38) M. Dinovitzer, X. Chen, J. Laliberte, X. Huang, and H. Frei, "Effect of wire and arc additive manufacturing (waam) process parameters on bead geometry and microstructure," *Addit. Manuf.*, **26** 138–146 (2019). doi:10.1016/j.addma.2018.12.013.